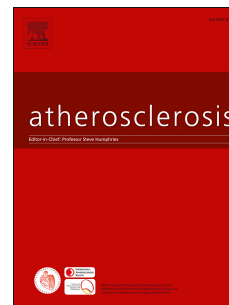


# Journal Pre-proof

Performance of a deep learning algorithm for the evaluation of CAD-RADS classification with CCTA

Giuseppe Muscogiuri, Mattia Chiesa, Michela Trotta, Marco Gatti, Vitanio Palmisano, Serena Dell'Aversana, Francesca Baessato, Annachiara Cavaliere, Gloria Cicala, Antonella Loffreno, Giulia Rizzon, Marco Guglielmo, Andrea Baggiano, Laura Fusini, Luca Saba, Daniele Andreini, Mauro Pepi, Mark G. Rabbat, Andrea I. Guaricci, Carlo N. De Cecco, Gualtiero Colombo, Gianluca Pontone



PII: S0021-9150(19)31607-7

DOI: <https://doi.org/10.1016/j.atherosclerosis.2019.12.001>

Reference: ATH 16141

To appear in: *Atherosclerosis*

Received Date: 21 August 2019

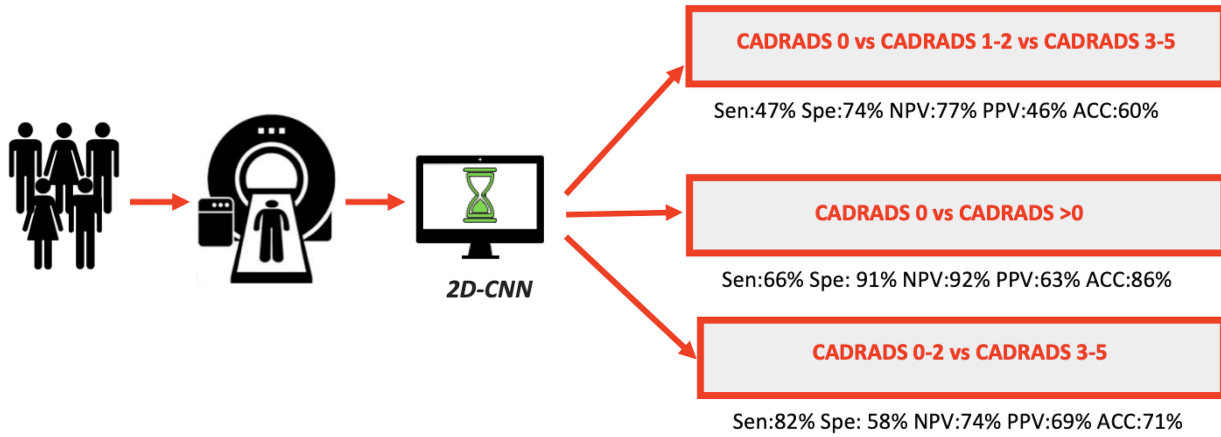
Revised Date: 1 December 2019

Accepted Date: 6 December 2019

Please cite this article as: Muscogiuri G, Chiesa M, Trotta M, Gatti M, Palmisano V, Dell'Aversana S, Baessato F, Cavaliere A, Cicala G, Loffreno A, Rizzon G, Guglielmo M, Baggiano A, Fusini L, Saba L, Andreini D, Pepi M, Rabbat MG, Guaricci AI, De Cecco CN, Colombo G, Pontone G, Performance of a deep learning algorithm for the evaluation of CAD-RADS classification with CCTA, *Atherosclerosis* (2020), doi: <https://doi.org/10.1016/j.atherosclerosis.2019.12.001>.

This is a PDF file of an article that has undergone enhancements after acceptance, such as the addition of a cover page and metadata, and formatting for readability, but it is not yet the definitive version of record. This version will undergo additional copyediting, typesetting and review before it is published in its final form, but we are providing this version to give early visibility of the article. Please note that, during the production process, errors may be discovered which could affect the content, and all legal disclaimers that apply to the journal pertain.

© 2019 Published by Elsevier B.V.



Journal Pre-proof

**Background and aims:** Artificial intelligence (AI) is increasing its role in diagnosis of patients with suspicious coronary artery disease. The aim of this manuscript is to develop a deep convolutional neural network (CNN) to classify coronary computed tomography angiography (CCTA) in the correct Coronary Artery Disease Reporting and Data System (CAD-RADS) category.

**Methods:** Two hundred eighty eight patients who underwent clinically indicated CCTA were included in this single-center retrospective study. The CCTAs were stratified by CAD-RADS scores by expert readers and considered as reference standard. A deep CNN was designed and tested on the CCTA dataset and compared to on-site reading. The deep CNN analyzed the diagnostic accuracy of the following three Models based on CAD-RADS classification: Model A (CAD-RADS 0 vs CAD-RADS 1-2 vs CAD-RADS 3,4,5), Model 1 (CAD-RADS 0 vs CAD-RADS>0), Model 2 (CAD-RADS 0-2 vs CAD-RADS 3-5). Time of analysis for both physicians and CNN were recorded.

**Results:** Model A showed a sensitivity, specificity, negative predictive value, positive predictive value and accuracy of 47%, 74%, 77%, 46% and 60%, respectively. Model 1 showed a sensitivity, specificity, negative predictive value, positive predictive value and accuracy of 66%, 91%, 92%, 63%, 86%, respectively. Conversely Model 2 demonstrated the following sensitivity, specificity, negative predictive value, positive predictive value and accuracy: 82%, 58%, 74%, 69%, 71%, respectively. Time of analysis was significantly lower using CNN as compared to on-site reading ( $530.5 \pm 179.1$  vs  $104.3 \pm 1.4$  seconds,  $p:0.01$ )

**Conclusions:** Deep CNN yielded accurate automated classification of patients with CAD-RADS.

## Performance of a deep learning algorithm for the evaluation of CAD-RADS classification with CCTA

<sup>1,\*</sup>Giuseppe Muscogiuri, MD, PhD, FSCCT, <sup>1,\*</sup>Mattia Chiesa, MSc, PhD, <sup>2</sup>Michela Trotta, MSc, <sup>3</sup>Marco Gatti, MD <sup>4</sup>Vitanio Palmisano, MD, <sup>5</sup>Serena Dell'Aversana, MD, <sup>6</sup>Francesca Baessato, MD <sup>7</sup>, Annachiara Cavaliere, MD, <sup>8</sup>Gloria Cicala, MD, <sup>9</sup>Antonella Loffreno, MD, <sup>7</sup>Giulia Rizzon, MD, <sup>1</sup>Marco Guglielmo, MD, FSCCT, <sup>1</sup>Andrea Baggiano, MD, <sup>1</sup>Laura Fusini, MD, <sup>4</sup>Luca Saba, MD, <sup>1,10</sup>Daniele Andreini, MD, PhD, FESC, FSCCT, <sup>1</sup>Mauro Pepi, MD, FESC, <sup>11,12</sup>Mark G. Rabbat, MD, <sup>13</sup>Andrea I. Guaricci, MD, PhD, FESC, <sup>14</sup>Carlo N. De Cecco, MD, PhD, <sup>1</sup>Gualtiero Colombo, MD <sup>1</sup>Gianluca Pontone MD, PhD, FESC, FSCCT

<sup>1</sup>Centro Cardiologico Monzino, IRCCS, Milan, Italy

<sup>2</sup> Department of Electrical, Computer and Biomedical Engineering, University of Pavia, Pavia, Italy

<sup>3</sup>Department of Surgical Sciences, Radiology Institute, University of Turin, Turin, Italy

<sup>4</sup> Department of Medical Imaging, University of Cagliari, Monserrato, Italy

<sup>5</sup> Department of Advanced Biomedical Sciences, University of Naples "Federico II", Naples, Italy

<sup>6</sup> Section of Cardiology, Department of Medicine, University of Verona, Verona, Italy

<sup>7</sup> Department of Medicine, Institute of Radiology, University of Padova, Padua, Italy

<sup>8</sup> Section of Radiology, Department of Medicine and Surgery, University of Parma, Parma, Italy

<sup>9</sup> Department of Cardiology, University of Insubria, Varese, Italy

<sup>10</sup> Department of Cardiovascular Sciences and Community Health, University of Milan

<sup>11</sup> Loyola University of Chicago, Chicago, IL, USA

<sup>12</sup> Edward Hines Jr. VA Hospital, Hines, IL, USA

<sup>13</sup> Institute of Cardiovascular Disease, Department of Emergency and Organ Transplantation, University Hospital "Policlinico Consorziale" of Bari, Bari, Italy

<sup>14</sup>Department of Radiology and Imaging Sciences, Emory University, Atlanta, GA, USA

\*: GM and MC contributed equally to this work

Numbers of figure: 5

Numbers of Tables: 6

Address for correspondence:

Gianluca Pontone, MD, PhD  
Centro Cardiologico Monzino, IRCCS  
Via Carlo Parea 4, 20138 Milan, Italy  
Phone: +39 0258002574  
E-mail: gianluca.pontone@ccfm.it

## Introduction

Cardiac computed tomography angiography (CCTA) is an excellent non-invasive technique for the assessment of stable coronary artery disease (CAD) <sup>1,2</sup>.

Thus application of CCTA in clinical practice is rapidly increasing especially considering its potential role as a gatekeeper for invasive coronary angiography<sup>3</sup>. Several classification systems for reporting of CCTA have been created with a recent introduction of CAD-RADS<sup>4</sup>.

In CAD-RADS classification the final score of CCTA is based on patient based analysis. Each vessel is evaluated using the following scale: 0=absence of CAD; 1=stenosis between 1-24%; 2= stenosis between 25-49%; 3=stenosis between 50-69%; 4=stenosis between 70-99% or >50% left main or three vessels >70%; 5=total occlusion; N=non diagnostic studies.

The CAD-RADS classification affords to have a simple classification for CAD, identifying patients that may require additional functional testing or invasive angiography.

Furthermore, CAD-RADS classification has a pivotal role in terms of prognosis. Indeed, as shown by Xie et al. patients with CAD-RADS 5 showed a 5 year event significantly higher compared with CAD-RADS 0 <sup>5</sup>.

Despite the majority of cardiac imaging interpretation and reporting being performed by readers, it is important to consider that machine learning or deep learning (DL) approaches may allow the evaluation of images in a short time compared to humans <sup>6</sup>. The application of artificial intelligence (AI) in cardiac imaging represents an interesting novelty in terms of both diagnosis and prognosis <sup>7</sup>.

Convolutional neural networks (CNN) are the most powerful Deep Learning technique used for diagnostic classification and prediction, starting from medical images <sup>8</sup>.

Considering the impact on clinical practice of CAD-RADS classification and the relative short time of analysis of the AI approach, we analyzed the effect of a novel CNN technique for CAD-RADS classification in patients referred for clinically indicated CCTA.

## Methods

### Study Population

We retrospectively analyzed the examinations of patients who underwent CCTA for clinical purposes from 2016 to 2018. Exclusion criteria were heart rate  $\geq 80$  bpm despite intravenous administration of beta blockers, atrial fibrillation and BMI  $\geq 35$  Kg/m<sup>2</sup>. The study was approved by the Institutional ethical committee. All patients provided written informed consent.

### CCTA Acquisition and Analysis

#### Patient preparation to CCTA and CCTA protocol

In patients with heart rate  $\geq 65$  bpm, without any contraindications to  $\beta$ -blockade therapy, metoprolol with a titration dose up to 25 mg was administered<sup>9</sup>. Sublingual nitrates were administered 5 minutes before the CCTA acquisition<sup>10</sup>.

CCTA acquisition was acquired using the following two CT scanners: Discovery CT 750 HD and Revolution CT (GE Healthcare, Milwaukee, IL). In the CCTA protocol of Discovery CT 750 HD, the following CT protocols were used: slice configuration 64 $\times$ 0.625 mm, with adapted tube current and tube voltage based on the BMI of patient<sup>11</sup>.

The CCTA protocol with the Revolution CT (GE Healthcare, Milwaukee, IL) was based on the following parameters: slice configuration 256 $\times$ 0.625 mm with tube current and tube voltage based on the BMI.

In both CT scanner protocol 50-70 ml of contrast medium (Iomeron 400 mg/mL, Bracco, Milan, Italy) was administered through the antecubital vein at an infusion rate of 5 mL/sec, followed by 50 mL of saline solution at the same infusion rate of contrast agent. In both CT scanners, CCTA was performed using the bolus tracking technique.

All images for both CT scanners were reconstructed using filtered back projection and in 75% or 40-80% of cardiac cycle based on the ECG-triggering acquisition used<sup>12</sup>. In selected cases with

poor image quality, the dataset was reconstructed by using intracycle motion correction as previously described<sup>12, 13</sup>.

### **Image quality analysis**

Subjective image quality was assessed by two cardiac imaging radiologists (VP and GM) with five and seven years of experience in cardiovascular imaging using the following four point Likert scale:

1= non-diagnostic, 2= adequate image quality, 3= good image quality; 4= excellent image quality.

Regarding objective image quality, the image noise was measured by manually drawing a region of interest (ROI) 20 mm in diameter in the aortic root, above the origin of the left main coronary artery (LM) and expressed as the standard deviation (SD) of vessel attenuation. Signal to noise ratio (SNR) for each coronary segment was calculated by dividing the coronary attenuation of proximal segments and image noise. Contrast to noise ratio (CNR) was obtained by dividing the difference between attenuation of coronary and surrounding tissue with the image noise<sup>14</sup>.

Coronary arteries were analyzed using the segmentation model according to the American Heart Association (AHA)<sup>15</sup>.

### **CAD-RADS score and coronary plaque evaluation**

The pool of CCTA examinations were reconstructed then analyzed in consensus by five different random couples between 10 radiologists and cardiologists (GP, MG, MG, AB, SD, GP, VP, GR, AC, DA). The experience of cardiac imagers involved in analysis ranged from 5 to 10 years. A CAD-RADS score was attributed for each examination. In cases of disagreement a cardiac imager (AIG) with ten years of experience in cardiovascular imaging adjudicated the final CAD-RADS score.

Based on composition of plaque, in patients with CADRADS >0, coronary plaques were identified and classified as calcified, mixed and soft in all vessels<sup>16</sup>.

Considering that CADRADS score is based on patient analysis, the burden of coronary artery disease of stenosis in other vessels was evaluated and classified according to the SCCT guidelines<sup>17</sup>.

According to the CADARADS classification the following three models were created: Model A= CADRADS 0 vs CADRADS 1-2 vs CADRADS 3-5. Subsequently two models were derived from Model A: Model 1 =(CADRADS 0 vs CADRADS 1-5) and Model 2 =(CADRADS 0-2 vs CADRADS 3-5). Time of analysis for each CCTA analysis of CNN and on-site reading were recorded and compared.

## **Deep learning methods**

### **Dataset generation**

Each CCTA scan was composed of 256 slices and stored in a DICOM format. For each sample, we removed the first 16 slices, selected the next (excluding the slices not representing the heart), placed them in an 11x11 squared image and resized each image to 512x512 pixels.

Axial images were provided to CNN algorithm in the same cardiac phase used for the clinical reporting. All CCTA images did not include any annotation.

Finally, to increase and balance the number of samples (100 in each class) and to reduce the overfitting, we performed the data augmentation strategy, rotating and zooming images<sup>18</sup>. At the end, the dataset was composed of 6 classes, each one of 100 samples.

### **CNN Architecture**

The 2D-CNN used in this study was designed after testing several combinations of hyperparameters. The keras R package in the framework of Tensorflow was used to build and test the CNN. The convolutional section of the network consisted of three consecutive layers of blocks, each one containing a sequence of three convolutional layers (32 filters 3 x 3 px)



and a max-pooling layer. Before each max-pooling layer, a batch normalization strategy was implemented to reduce the overfitting of the training model <sup>19</sup>. Each convolutional layer was composed of 32 filters (3 x 3 px) and the pooling windows size was 2 x 2. The number of neurons in the output layer corresponded to the number of classes in a specific classification analysis. To handle the overfitting a dropout strategy was implemented before the first hidden layer (dropout rate: 0.5) <sup>19</sup>. The ReLU activation function <sup>19</sup> was used for each neuron (densely connected and convolutional ones), except for the output layer ones (activation function: 'softmax'). Finally, we used the Back Propagation optimizer to minimize the categorical cross entropy and implemented the 'early stopping' strategy as a regularization method to prevent overfitting. The designed CNN is sketched in Figure 1.

The main endpoints of the study were:

- a) Evaluation of diagnostic accuracy of CNN for differentiation between Model A, Model 1 and Model 2.
- b) Univariate and multivariate analysis for identification of predictive factors for failure of CNN were analysed.
- c) Comparison of time of analysis between the CNN approach versus on-site reading.

### **Statistical analysis**

To evaluate the overall classification performance a 5-fold Cross Validation was implemented (Figure 2). For each iteration, a training set is generated, combining four folds (80 samples per class); the remaining fold (20 samples per class) was used as test set. The training set is used to learn the CNN parameters (Figure 3, supplemental material), while on the test set the standard evaluation metrics (i.e., sensitivity, specificity, negative predicted value, positive predicted value, and accuracy, and the area under the curve) are calculated.

Intra- and inter-observer reliability were calculated using the kappa score by considering all subjects and by splitting subjects by class.

Univariate and multivariate logistic regression analyses were used to identify independent factors associated with a CNN misreading of the CAD-RADS score. A p-value  $< 0.05$  was considered significant. Statistical analysis was performed using SPSS 25 (SPSS Inc, Chicago, IL) and R version 3.5.1 (R Foundation for Statistical Computing, Vienna, Austria).

Journal Pre-proof

## Results

Two hundred eighty eight examinations were evaluated (CADRADS 0: 50 exams; CADRADS 1: 50 exams; CADRADS 2: 50 exams; CADRADS 3: 50 exams; CADRADS 4: 50 exams; CADRADS 5: 38 exams). Two example cases of CADRADS 0 and CADRADS 5 are summarized in Figure 4.

The baseline characteristics of the overall population were summarized in Table 1.

The subjective image quality was good for all coronary segments showing a high inter-reader and intra-reader reproducibility Tables 2 and 3 (supplemental material).

The diagnostic accuracy of the 2D-CNN approach was analyzed for Model A demonstrating a sensitivity, specificity, negative predictive value, positive predictive value and accuracy of 47% (20-74%), 74% (54-94%), 77% (68-86%), 46% (31-61%) and 60% (54-66%), respectively.

From Model A, two further models were derived, Model 1 and Model 2, showing a sensitivity, specificity, negative predictive value, positive predictive value, accuracy and area under curve of 66% (53-79%), 91% (54-94%), 92% (89-96%), 63% (50-75%), 86% (82-90%), 89% (84-94%), respectively and 82% (76-88%), 58% (50-67%), 74% (66-82%), 69% (63-76%), 71% (66-76%), 78% (75-82%), respectively. The results concerning Model 1 and 2 are summarized in Table 4 and Figure 5.

On multivariate analysis, the analysis tailored for plaque analysis showed on multivariate analysis, that plaque characteristics, degree of stenosis as well as subjective image quality did not influence the predictive value of Model A (Table 5).

Considering that plaque imaging did not influence the diagnostic accuracy in Model A we focused on plaque imaging in derived Model 1 and Model 2.

Regarding Models 1 and 2, multivariate analysis showed that presence of plaque, regardless of the composition, was an independent predictor of success in Model 1; conversely, in Model 2, the presence of stenosis >50% was a predictor of failure (Tables 6).

After the evaluation of CCTA image quality and diagnostic accuracy of 2D CNN we analyzed the impact of time consumed in terms of CAD-RADS classification and we observed that time of analysis was significantly higher ( $p= 0.01$ ) for on-site physicians reading as compared to the CNN approach ( $530.5\pm 179.1$  vs.  $104.3\pm 1.4$  seconds,  $p:0.01$ ).

## Discussion

Our study is the first to describe the application of AI for CADRADS classification. In clinical practice, it is important to correctly identify the CADRADS category. Patients in CADRADS 0 do not appear to derive benefit from medical therapy, while patients with CADRADS 1-2 may have benefit by medical treatment and patients with CADRADS 3-5 may necessitate further testing of ischemia or invasive coronary angiography. The main results of our study are that Model A did not show a good diagnostic accuracy and area under curve, therefore the 2D CNN approach seems to have poor diagnostic accuracy if the model includes the three classes. A more simplified approach of CAD-RADS classification was shown in Model 1 and Model 2. Model 1 was composed by two subgroups of patients that differ for clinical management based on CCTA results. Contrary to Model A, Model 1 showed good diagnostic accuracy for detection of patients positive and negative for presence of CAD regardless of plaque composition and grade of stenosis. Finally, Model 2 was composed of two subgroups that mainly differ on the therapeutic approach after the results of CCTA. In the subgroup of CADRADS 0-2, patients may derive benefit of medical therapy while the subgroup of

CADRADS 3-5 may have benefit from further tests of ischemia or invasive coronary angiography<sup>20</sup>. Compared to Model 1, Model 2 showed a lower diagnostic accuracy and AUC with a high degree of stenosis as a major independent predictor of misclassification.

Nowadays the non-invasive assessment of CAD is mainly focused on evaluation of calcium score (CS) and CCTA. Both CS and CCTA provide information useful for planning of treatment strategy and prognostic stratification; therefore, considering the pivotal role of these CT acquisitions a ML approach has been developed<sup>7, 21</sup>. Artificial intelligence, similar to our manuscript, appears to be important for the diagnosis of CAD<sup>22</sup>, furthermore using some algorithms it is possible also to provide information concerning CAD in non-gated CT images<sup>23</sup>.

Moving on details, Takx et al. described the possibility to evaluate CS using non-contrast, non-gated CT using a low dose protocol<sup>23</sup>. In particular Takx and colleagues using a supervised pattern recognition system k-nearest neighbor with support vector machine classifiers for identification of CS demonstrated a good reliability when compared with CS calculated by manual delineation<sup>23</sup>.

One of the application of AI in CCTA was shown by Kang et colleagues<sup>22</sup>. The authors using a two-step ML approach which incorporated a support vector machine, demonstrated a sensitivity, specificity, accuracy and AUC of 93%; 95%, 94% and 94% in diagnosing CAD. This promising technique did not differentiate the entity of CAD furthermore and the authors did not specify the time spent for each analysis<sup>22</sup>. Another interesting technique for the evaluation of CAD in CCTA using an automated algorithm was described by Dey et al.<sup>24</sup>. The authors quantified the non-calcified and calcified plaque using an automated algorithm and discovered a good agreement when compared with human evaluation<sup>24</sup>.

The aforementioned manuscripts regarding the application of AI in diagnostic pathway of CAD differ by the algorithm of AI used. Despite in our manuscript we used the 2D CNN

approach unlike the others articles that used different algorithms of AI we have in common the main purpose represented by the simplification of diagnostic pathway.

Despite the aforementioned studies analyzing the impact of AI in cardiac imaging, none of them evaluate its role in CADRADS classification.

In this article, the main finding is represented by the ability of CNN to differentiate with high diagnostic accuracy patients with CADRADS 0 and CADRADS>0.

Based on results of our manuscript, it may be possible to use a CNN algorithm in clinical practice and rule out the presence of CAD in a relatively short time. Considering that the prevalence of normal coronaries is high in patients even with an increased pretest probability<sup>25, 26</sup> it is plausible that CCTA interpretation may be accelerated by the application of CNN algorithms as shown in Figure 6.

Another important finding is the possibility to correctly predict with high diagnostic accuracy Models 1 and 2, independently of the image quality of CCTA acquisition. Indeed both SNR and CNR do not appear to influence CADRADS classification using CNN. The latter finding is important, especially when employing low dose CCTA protocols.

Some limitations should be mentioned in this manuscript.

First, a small sample size was used for the study. A larger, multicenter study, involving a larger sample size may increase the diagnostic accuracy in all three models used in the manuscript.

Second, we speculate that for Model 1, the CNN approach was able to better identify patients with plaque because an increase in CADRADS score is correlated with more calcified and soft plaque and subsequently a larger amount of data for the training set.

Third, most of the CCTA were acquired using the latest generation CT, therefore it is important to consider that the application of CNN algorithms may provide different results with poor image quality.

In conclusion, this new CNN approach can be helpful for identification of patients with CADRADS 0 in a short time of analysis using a good image quality dataset. Further studies with a larger population need to be performed in order to improve the diagnostic accuracy of CNN.

**Conflicts of interest:** All authors guarantee that have not conflicts of interest.

**Authors contribution:**

GM,LS,DA,MP,MGR,AIG,CNDC,GC and GP revised the manuscript.MC and MT developed the CNN.MG,VP,SDA,FC,AC,GC,AL,GR,MG,AB,LF selected and analyzed the images.

## References

1. Pontone G, Andreini D, Bartorelli AL, Cortinovis S, Mushtaq S, Bertella E, Annoni A, Formenti A, Nobili E, Trabattoni D, Montorsi P, Ballerini G, Agostoni P and Pepi M. Diagnostic accuracy of coronary computed tomography angiography: a comparison between prospective and retrospective electrocardiogram triggering. *J Am Coll Cardiol*. 2009;54:346-55.
2. Pontone G, Andreini D, Bartorelli AL, Bertella E, Cortinovis S, Mushtaq S, Foti C, Annoni A, Formenti A, Baggiano A, Conte E, Bovis F, Veglia F, Ballerini G, Fiorentini C, Agostoni P and Pepi M. A long-term prognostic value of CT angiography and exercise ECG in patients with suspected CAD. *JACC Cardiovasc Imaging*. 2013;6:641-50.
3. Pontone G, Baggiano A, Andreini D, Guaricci AI, Guglielmo M, Muscogiuri G, Fusini L, Fazzari F, Mushtaq S, Conte E, Calligaris G, De Martini S, Ferrari C, Galli S, Grancini L, Ravagnani P, Teruzzi G, Trabattoni D, Fabbicchi F, Lualdi A, Montorsi P, Rabbat MG, Bartorelli AL and Pepi M. Stress Computed Tomography Perfusion Versus Fractional Flow Reserve CT Derived in Suspected Coronary Artery Disease: The PERFECTION Study. *JACC Cardiovasc Imaging*. 2019;12:1487-1497.
4. Cury RC, Abbara S, Achenbach S, Agatston A, Berman DS, Budoff MJ, Dill KE, Jacobs JE, Maroules CD, Rubin GD, Rybicki FJ, Schoepf UJ, Shaw LJ, Stillman AE, White CS, Woodard PK and Leipsic JA. CAD-RADS(TM) Coronary Artery Disease - Reporting and Data System. An expert consensus document of the Society of Cardiovascular Computed Tomography (SCCT), the American College of Radiology (ACR) and the North American Society for Cardiovascular Imaging (NASCI). Endorsed by the American College of Cardiology. *J Cardiovasc Comput Tomogr*. 2016;10:269-81.
5. Xie JX, Cury RC, Leipsic J, Crim MT, Berman DS, Gransar H, Budoff MJ, Achenbach S, B OH, Callister TQ, Marques H, Rubinshtein R, Al-Mallah MH, Andreini D, Pontone G, Cademartiri F, Maffei E, Chinnaiyan K, Raff G, Hadamitzky M, Hausleiter J, Feuchtner G, Dunning A, DeLago A, Kim YJ, Kaufmann PA, Villines TC, Chow BJW, Hindoyan N, Gomez M, Lin FY, Jones E, Min JK and Shaw LJ. The Coronary Artery Disease-Reporting and Data System (CAD-RADS): Prognostic and Clinical Implications Associated With Standardized Coronary Computed Tomography Angiography Reporting. *JACC Cardiovasc Imaging*. 2018;11:78-89.
6. Chartrand G, Cheng PM, Vorontsov E, Drozdal M, Turcotte S, Pal CJ, Kadoury S and Tang A. Deep Learning: A Primer for Radiologists. *Radiographics*. 2017;37:2113-2131.
7. Al'Aref SJ, Anchouche K, Singh G, Slomka PJ, Kolli KK, Kumar A, Pandey M, Maliakal G, van Rosendaal AR, Beecy AN, Berman DS, Leipsic J, Nieman K, Andreini D, Pontone G, Schoepf UJ, Shaw LJ, Chang HJ, Narula J, Bax JJ, Guan Y and Min JK. Clinical applications of machine learning in cardiovascular disease and its relevance to cardiac imaging. *Eur Heart J*. 2018.
8. Litjens G, Kooi T, Bejnordi BE, Setio AAA, Ciompi F, Ghafoorian M, van der Laak J, van Ginneken B and Sanchez CI. A survey on deep learning in medical image analysis. *Med Image Anal*. 2017;42:60-88.
9. Pontone G, Muscogiuri G, Andreini D, Guaricci AI, Guglielmo M, Baggiano A, Fazzari F, Mushtaq S, Conte E, Annoni A, Formenti A, Mancini E, Verdecchia M, Campari A, Martini C, Gatti M, Fusini L, Bonfanti L, Consiglio E, Rabbat MG, Bartorelli AL and Pepi M. Impact of a New Adaptive Statistical Iterative Reconstruction (ASIR)-V Algorithm on Image Quality in Coronary Computed Tomography Angiography. *Acad Radiol*. 2018;25:1305-1313.
10. Takx RA, Sucha D, Park J, Leiner T and Hoffmann U. Sublingual Nitroglycerin Administration in Coronary Computed Tomography Angiography: a Systematic Review. *Eur Radiol*. 2015;25:3536-42.



11. Pontone G, Andreini D, Bartorelli AL, Bertella E, Mushtaq S, Foti C, Formenti A, Chiappa L, Annoni A, Cortinovis S, Baggiano A, Conte E, Bovis F, Veglia F, Ballerini G, Agostoni P, Fiorentini C and Pepi M. Feasibility and diagnostic accuracy of a low radiation exposure protocol for prospective ECG-triggering coronary MDCT angiography. *Clin Radiol*. 2012;67:207-15.
12. Pontone G, Muscogiuri G, Baggiano A, Andreini D, Guaricci AI, Guglielmo M, Fazzari F, Mushtaq S, Conte E, Annoni A, Formenti A, Mancini E, Verdecchia M, Fusini L, Bonfanti L, Consiglio E, Rabbat MG, Bartorelli AL and Pepi M. Image Quality, Overall Evaluability, and Effective Radiation Dose of Coronary Computed Tomography Angiography With Prospective Electrocardiographic Triggering Plus Intracycle Motion Correction Algorithm in Patients With a Heart Rate Over 65 Beats Per Minute. *J Thorac Imaging*. 2018;33:225-231.
13. Pontone G, Andreini D, Bertella E, Baggiano A, Mushtaq S, Loguercio M, Segurini C, Conte E, Beltrama V, Annoni A, Formenti A, Petulla M, Guaricci AI, Montorsi P, Trabattoni D, Bartorelli AL and Pepi M. Impact of an intra-cycle motion correction algorithm on overall evaluability and diagnostic accuracy of computed tomography coronary angiography. *Eur Radiol*. 2016;26:147-56.
14. Pflederer T, Rudofsky L, Ropers D, Bachmann S, Marwan M, Daniel WG and Achenbach S. Image quality in a low radiation exposure protocol for retrospectively ECG-gated coronary CT angiography. *AJR Am J Roentgenol*. 2009;192:1045-50.
15. Austen WG, Edwards JE, Frye RL, Gensini GG, Gott VL, Griffith LS, McGoon DC, Murphy ML and Roe BB. A reporting system on patients evaluated for coronary artery disease. Report of the Ad Hoc Committee for Grading of Coronary Artery Disease, Council on Cardiovascular Surgery, American Heart Association. *Circulation*. 1975;51:5-40.
16. Cademartiri F, Romano M, Seitun S, Maffei E, Palumbo A, Fusaro M, Aldrovandi A, Messalli G, Tresoldi S, Malago R, La Grutta L, Runza G, Brambilla V, Tedeschi C, Casolo G, Midiri M and Mollet NR. Prevalence and characteristics of coronary artery disease in a population with suspected ischemic heart disease using CT coronary angiography: correlations with cardiovascular risk factors and clinical presentation. *Radiol Med*. 2008;113:363-72.
17. Leipsic J, Abbara S, Achenbach S, Cury R, Earls JP, Mancini GJ, Nieman K, Pontone G and Raff GL. SCCT guidelines for the interpretation and reporting of coronary CT angiography: a report of the Society of Cardiovascular Computed Tomography Guidelines Committee. *J Cardiovasc Comput Tomogr*. 2014;8:342-58.
18. Pereira S, Pinto A, Alves V and Silva CA. Brain Tumor Segmentation Using Convolutional Neural Networks in MRI Images. *IEEE Trans Med Imaging*. 2016;35:1240-1251.
19. Nirschl JJ, Janowczyk A, Peyster EG, Frank R, Margulies KB, Feldman MD and Madabhushi A. A deep-learning classifier identifies patients with clinical heart failure using whole-slide images of H&E tissue. *PLoS One*. 2018;13:e0192726.
20. Pontone G, Andreini D, Guaricci AI, Baggiano A, Fazzari F, Guglielmo M, Muscogiuri G, Berzovini CM, Pasquini A, Mushtaq S, Conte E, Calligaris G, De Martini S, Ferrari C, Galli S, Grancini L, Ravagnani P, Teruzzi G, Trabattoni D, Fabbicchi F, Lualdi A, Montorsi P, Rabbat MG, Bartorelli AL and Pepi M. Incremental Diagnostic Value of Stress Computed Tomography Myocardial Perfusion With Whole-Heart Coverage CT Scanner in Intermediate- to High-Risk Symptomatic Patients Suspected of Coronary Artery Disease. *JACC Cardiovasc Imaging*. 2019;12:338-349.
21. Singh G, Al'Aref SJ, Van Assen M, Kim TS, van Rosendaal A, Kolli KK, Dwivedi A, Maliakal G, Pandey M, Wang J, Do V, Gummalla M, De Cecco CN and Min JK. Machine learning in cardiac CT: Basic concepts and contemporary data. *J Cardiovasc Comput Tomogr*. 2018;12:192-201.
22. Kang D, Dey D, Slomka PJ, Arsanjani R, Nakazato R, Ko H, Berman DS, Li D and Kuo CC. Structured learning algorithm for detection of nonobstructive and obstructive coronary plaque lesions from computed tomography angiography. *J Med Imaging (Bellingham)*. 2015;2:014003.

23. Takx RA, de Jong PA, Leiner T, Oudkerk M, de Koning HJ, Mol CP, Viergever MA and Isgum I. Automated coronary artery calcification scoring in non-gated chest CT: agreement and reliability. *PLoS One*. 2014;9:e91239.
24. Dey D, Cheng VY, Slomka PJ, Nakazato R, Ramesh A, Gurudevan S, Germano G and Berman DS. Automated 3-dimensional quantification of noncalcified and calcified coronary plaque from coronary CT angiography. *J Cardiovasc Comput Tomogr*. 2009;3:372-82.
25. Chow BJ, Small G, Yam Y, Chen L, Achenbach S, Al-Mallah M, Berman DS, Budoff MJ, Cademartiri F, Callister TQ, Chang HJ, Cheng V, Chinnaiyan KM, Delago A, Dunning A, Hadamitzky M, Hausleiter J, Kaufmann P, Lin F, Maffei E, Raff GL, Shaw LJ, Villines TC, Min JK and Investigators C. Incremental prognostic value of cardiac computed tomography in coronary artery disease using CONFIRM: COroNary computed tomography angiography evaluation for clinical outcomes: an InteRnational Multicenter registry. *Circ Cardiovasc Imaging*. 2011;4:463-72.
26. Foldyna B, Udelson JE, Karady J, Banerji D, Lu MT, Mayrhofer T, Bittner DO, Meyersohn NM, Emami H, Genders TSS, Fordyce CB, Ferencik M, Douglas PS and Hoffmann U. Pretest probability for patients with suspected obstructive coronary artery disease: re-evaluating Diamond-Forrester for the contemporary era and clinical implications: insights from the PROMISE trial. *Eur Heart J Cardiovasc Imaging*. 2018.

## Figures

**Figure 1.** Graphical sketch of the designed CNN architecture. Three consecutive convolutional blocks, each one composed of 3 convolutional layers (light blue squares) and a max pooling layer (green square), are followed by a densely connected network (2 hidden layers (violet squares) and an output layer (yellow square)). During the CNN training, some neurons are dropped out (red crossed circles) and others are active (blue circles).

**Figure 2.** Overview of the deep learning analysis. First, the whole dataset was split in 5 folds, each one composed of 20 samples per class. Then, a cross validation procedure was implemented: 4 folds were selected to train the CNN (training set) and build the model; the fifth fold was used to test the learned model (test set) and to assess the performance.

**Figure 3:** Figure representing the input image provided to the 2D-CNN.

**Figure 4.** A 53-year-old woman with family history of cardiovascular disease, palpitations and dyspnea. CAD RADS 0: (A) Absence of pathology in left anterior descending artery, (B) circumflex artery and (C) right coronary artery.

A 67-year-old man with dyslipidemia and severe left ventricular dysfunction by echocardiography. CAD RADS 5: (D) Severe stenosis of the proximal left anterior descending artery, (E) absence of pathology of circumflex artery and (F) occlusion of mid portion of right coronary artery (arrow).

**Figure 5.** Receiver operating characteristic curve (ROC) showing the predictive accuracy of Convolutional Neural Networks to distinguish between CADRADS 0, CADRADS>0 (Model 1) and CADRADS 0-2, CADRADS 3-5 (Model 2).

**Figure 6.** Simulation of the diagnostic algorithm in a clinical setting using CNN for CADRADS classification.

## Tables

**Table 1.** Baseline Characteristics of the Overall Population

**Table 2.** Comparison of Image Quality of all classes of patients by Readers 1 and 2.

**Table 3.** Comparison of Image Quality of all classes of patients by the same Reader in two different lectures

**Table 4.** Diagnostic accuracy for Model 1 and Model 2

**Table 5.** Univariate Analysis for Model A

**Table 6.** Univariate and Multivariate analysis for Model 1 and Model 2

**Table 1.** Baseline characteristics of the overall population

Characteristics	Values
Number, <i>n</i>	288
Age (y), mean $\pm$ SD	60.6 $\pm$ 12.4
Male, <i>n</i> (%)	198 (69)
Body mass index (kg/m <sup>2</sup> ), mean $\pm$ SD	25.8 $\pm$ 4.5
Risk factors	
Hypertension, <i>n</i> (%)	96 (33)
Smoker, <i>n</i> (%)	46 (16)
Hyperlipidemia, <i>n</i> (%)	86 (30)
Diabetes, <i>n</i> (%)	21 (7)
Family history, <i>n</i> (%)	96 (33)
Clinical history	
Chest pain, <i>n</i> (%)	65 (23)
Dyspnea, <i>n</i> (%)	15 (5)
Palpitation, <i>n</i> (%)	4 (1)
Positive stress test, <i>n</i> (%)	31 (10)
Follow-up of known CAD, <i>n</i> (%)	35 (12)
Valvular disease, <i>n</i> (%)	12 (4)
Arrhythmias, <i>n</i> (%)	43 (15)
Dilated cardiomyopathy, <i>n</i> (%)	6 (2)
Intravenous $\beta$ -blocker	
Number of patients, <i>n</i> (%)	155 (54)
Dose (mg), mean $\pm$ SD	9.8 $\pm$ 4.7
Heart rate during the scan	
Minimum heart rate (bpm), mean $\pm$ SD	55.4 $\pm$ 9.6
Mean heart rate (bpm), mean $\pm$ SD	60.6 $\pm$ 10.5
Maximum heart rate (bpm), mean $\pm$ SD	74.4 $\pm$ 31.7
Radiation exposure	
Dose length product, mean $\pm$ SD	264.9 $\pm$ 125.5

CAD, coronary artery disease; SD, standard deviation.

**Table 2.** Comparison of Image Quality of all classes of patients by Readers 1 and 2.

	All classes		
	Reader 1	Reader 2	Cohen's Kappa
LM	3.2 ± 0.5	3.6 ± 0.5	0.93
Proximal_LAD	3.6 ± 0.5	3.6 ± 0.5	0.89
Mid_LAD	3.5 ± 0.6	3.5 ± 0.6	0.90
Distal_LAD	3.2 ± 0.8	3.1 ± 0.8	0.90
LAD	3.5 ± 0.6	3.5 ± 0.6	0.92
D1	2.9 ± 0.7	2.9 ± 0.7	0.89
Proximal_LCX	3.3 ± 0.6	3.3 ± 0.6	0.93
Mid_LCX	3.2 ± 0.7	3.2 ± 0.6	0.92
Distal_LCX	2.8 ± 0.8	2.8 ± 0.8	0.89
LCX	3.1 ± 0.6	3.1 ± 0.6	0.94
M1	2.8 ± 0.8	2.8 ± 0.8	0.93
Proximal_RCA	3.5 ± 0.6	3.5 ± 0.6	0.95
Mid_RCA	3.5 ± 0.6	3.5 ± 0.7	0.95
Distal_RCA	3.4 ± 0.7	3.4 ± 0.7	0.96
RCA	3.5 ± 0.6	3.5 ± 0.6	0.97
PLA	3.4 ± 0.6	3.3 ± 0.6	0.93
PDA	3.3 ± 0.7	3.3 ± 0.7	0.93
Patient	3.4 ± 0.6	3.4 ± 0.6	0.93

LM, left main coronary; LAD, anterior descending artery; D1, first diagonal artery; LCX, circumflex artery; M1, first obtuse marginal branch; RCA, right coronary artery, PLA, postero-lateral branch; PDA, posterior descending artery.

**Table. 3** Comparison of Image Quality of all classes of patients by the same Reader in two different lectures

	All classes		
	First Lecture	Second Lecture	Cohen's Kappa
LM	3.2 ± 0.5	3.6 ± 0.5	0.90
Proximal_LAD	3.6 ± 0.5	3.6 ± 0.5	0.87
Mid_LAD	3.5 ± 0.6	3.5 ± 0.6	0.85
Distal_LAD	3.2 ± 0.8	3.1 ± 0.8	0.86
LAD	3.5 ± 0.6	3.5 ± 0.6	0.87
D1	2.9 ± 0.7	3.0 ± 0.7	0.86
Proximal_LCX	3.3 ± 0.6	3.3 ± 0.6	0.95
Mid_LCX	3.2 ± 0.7	3.1 ± 0.7	0.93
Distal_LCX	2.8 ± 0.8	2.7 ± 0.8	0.87
LCX	3.1 ± 0.6	3.1 ± 0.6	0.93
M1	2.8 ± 0.8	2.8 ± 0.8	0.91
Proximal_RCA	3.5 ± 0.6	3.5 ± 0.6	0.93
Mid_RCA	3.5 ± 0.6	3.5 ± 0.6	0.94
Distal_RCA	3.4 ± 0.7	3.4 ± 0.7	0.93
RCA	3.5 ± 0.6	3.5 ± 0.6	0.94
PLA	3.4 ± 0.6	3.3 ± 0.6	0.88
PDA	3.3 ± 0.7	3.2 ± 0.7	0.88
Patient	3.4 ± 0.6	3.4 ± 0.6	0.93

LM, left main coronary; LAD, anterior descending artery; D1, first diagonal artery; LCX, circumflex artery; M1, first obtuse marginal branch; RCA, right coronary artery, PLA, postero-lateral branch; PDA, posterior descending artery.

**Table 4.** Diagnostic accuracy for Model 1 and Model 2

	<b>Model 1 (95%CI)</b>	<b>Model 2 (95%CI)</b>
Sensitivity	66% (53-79%)	82% (76-88%)
Specificity	91% (87-95%)	58% (50-67%)
Positive predictive value	63% (50-75%)	69% (63-76%)
Negative predictive value	92% (89-96%)	74% (66-82%)
Accuracy	86% (82-90%)	71% (66-76%)
Area under curve	89% (84-94%)	78% (75-82%)
True positive	35	125
False positive	21	159
True negative	210	77
False negative	18	27

Model 1, CAD-RADS 0 vs CAD-RADS 1-5; Model 2, CAD-RADS 0-2 vs CAD-RADS 3-5



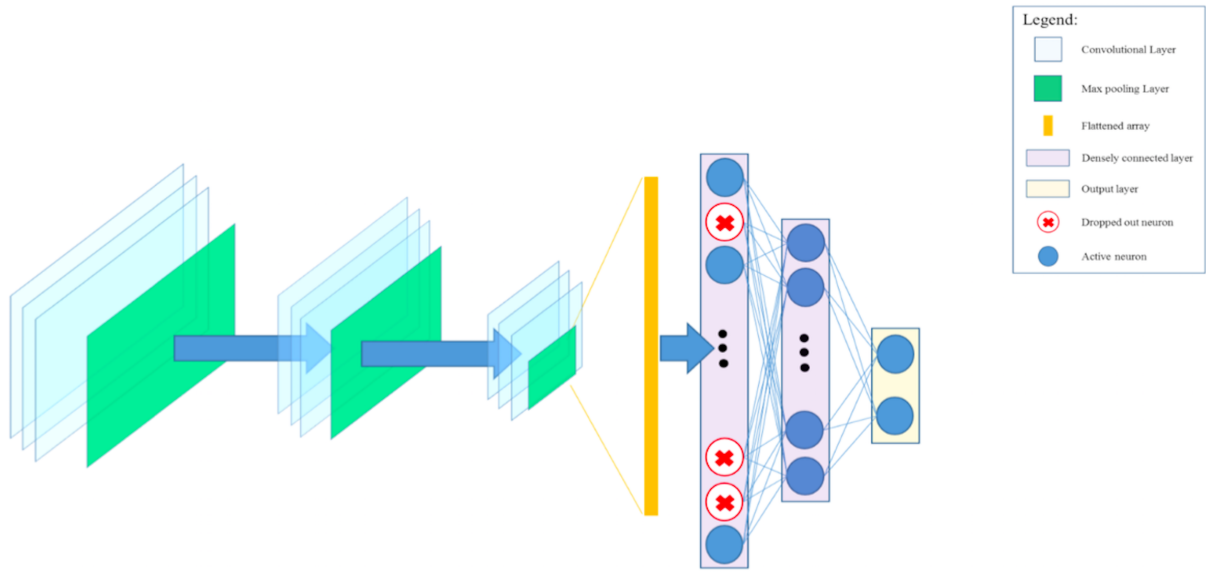
**Table 5.** Univariate analysis for model A

CADRADS 0 vs CADRADS 1-2 vs CADRADS 3-5	Univariate	
	OR (95%CI)	p Value
BMI	1.021(0.966-1.08)	0.455
Mean HR	0.992(0.969-1.017)	0.542
Plaques		
No plaques	-	-
Fibrotic	1.136(0.450-2.867)	0.787
Calcific	1.617(0.844-3.099)	0.147
Stenosis > 50%	1.269(0.743-2.057)	0.333
SNR	1.028(0.957-1.104)	0.447
CNR	1.020(0.95-1.094)	0.588

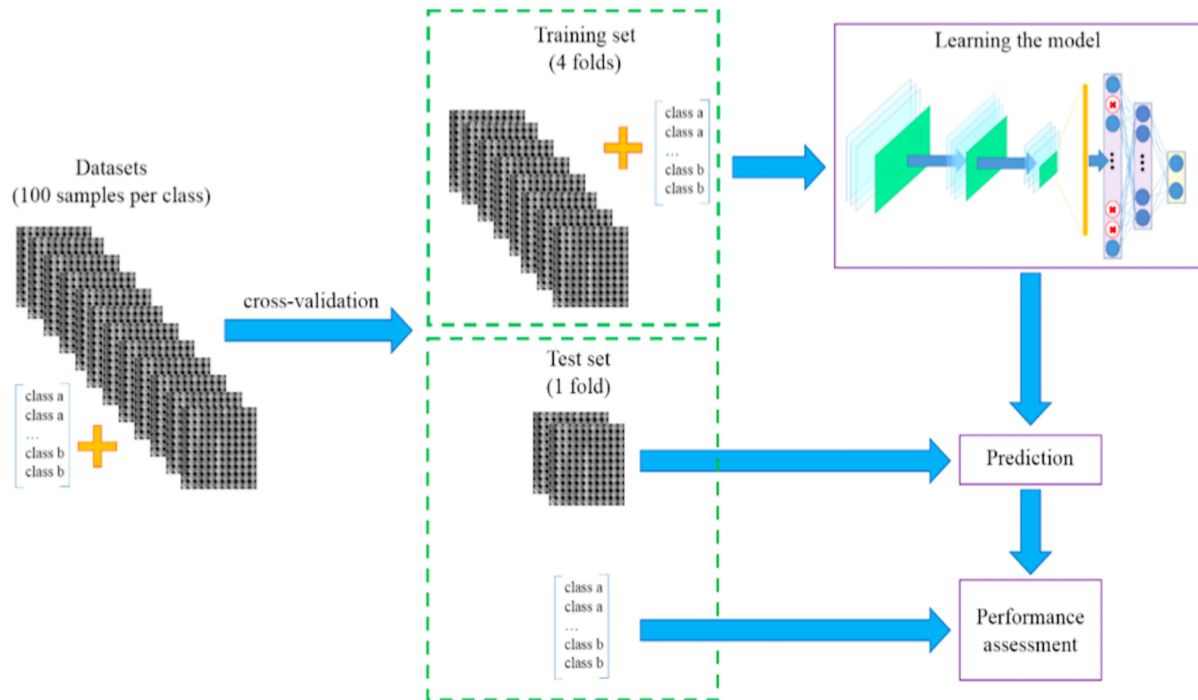
BMI, body mass index; HR, heart rate; SNR, signal to noise ratio; CNR, contrast to noise ratio

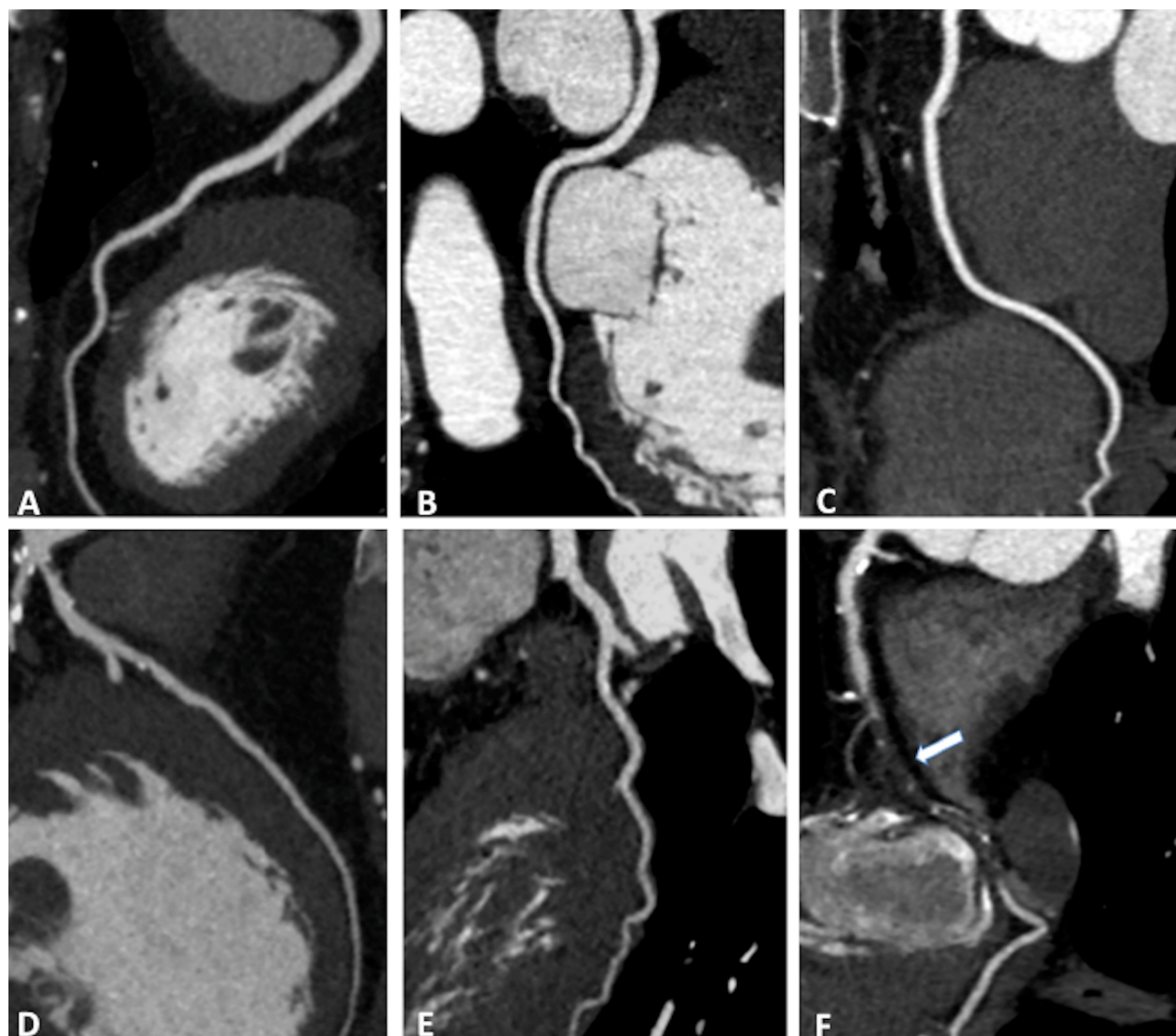
**Table 6.** Univariate and multivariate analysis for Model 1 and 2

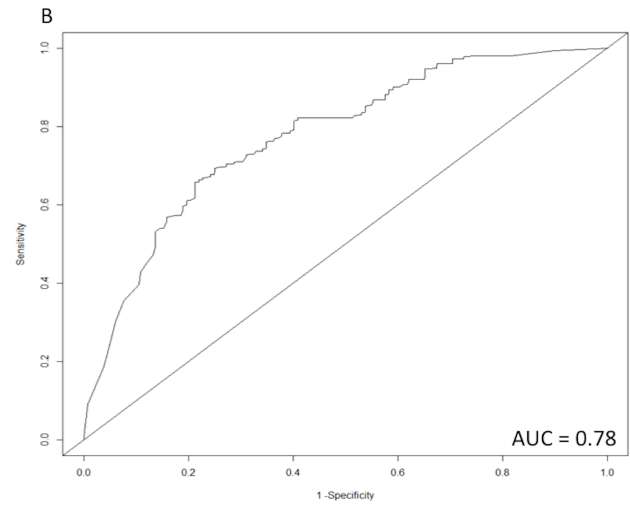
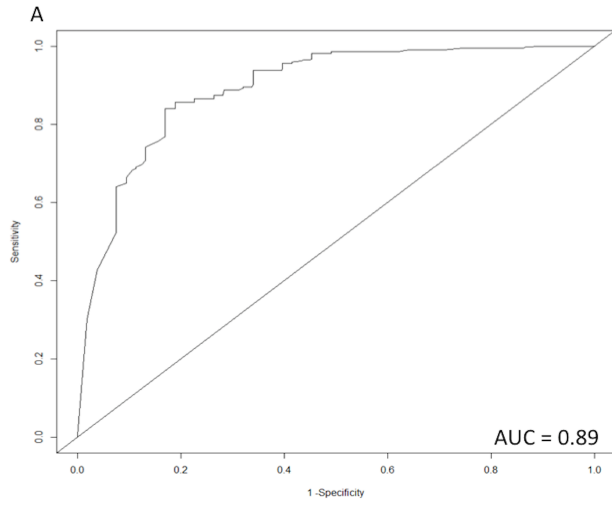
<b>Model 1 (CAD-RADS 0 vs CAD-RADS 1-5)</b>				
	<b>Univariate</b>		<b>Multivariate</b>	
	<b>OR (95%CI)</b>	<b>p Value</b>	<b>OR (95%CI)</b>	<b>p Value</b>
BMI	0.987(0.909-1.073)	0.762		
Mean HR	0.995(0.962-1.03)	0.775		
Plaques				
No plaque	-	-	-	-
Fibrotic	<b>0.125(0.027-0.581)</b>	<b>0.008</b>	0.142(0.030-0.671)	0.014
Calcific	<b>0.216(0.103-0.451)</b>	<b>&lt;0.001</b>	0.291(0.121-0.701)	0.002
Stenosis > 50%	<b>0.351(0.164-0.751)</b>	<b>0.007</b>	0.592(0.236-1.481)	0.262
SNR	1.066(0.968-1.175)	0.196		
CNR	1.064(0.967-1.171)	0.202		
<b>Model 2 (CAD-RADS 0-2 vs CAD-RADS 3-5)</b>				
	<b>Univariate</b>		<b>Multivariate</b>	
	<b>OR (95%CI)</b>	<b>p Value</b>	<b>OR (95%CI)</b>	<b>p Value</b>
BMI	1.038(0.979-1.100)	0.217		
Mean HR	0.998(0.973-1.024)	0.893		
Plaque				
No plaque	-	-	-	-
Fibrotic	2.074(0.632-6.804)	0.229	1.511(0.445-5.132)	0.508
Calcific	<b>4.381(1.785-10.754)</b>	<b>0.001</b>	2.420(0.896-6.534)	0.081
Stenosis > 50%	<b>3.350(1.949-5.759)</b>	<b>&lt;0.001</b>	2.476(1.349-4.543)	0.003
SNR	0.984(0.911-1.063)	0.684		
CNR	0.980(0.909-1.058)	0.606		
BMI, body mass index; HR, heart rate; SNR, signal to noise ratio; CNR, contrast to noise ratio				



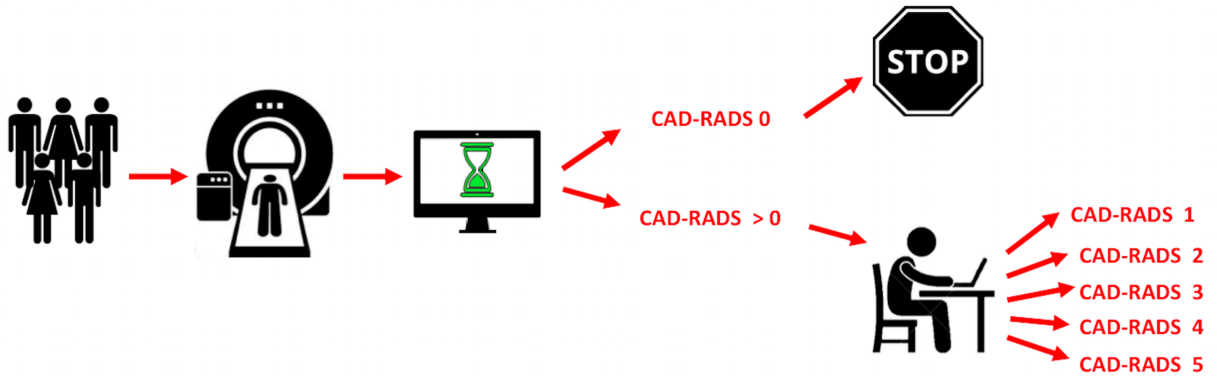
Journal Pre-proof







Journal Pre-proof



Journal Pre-proof

- Deep CNN yielded accurate automated CAD-RADS classification in patients with suspicious CAD.
- CAD-RADS classification is significant faster compared to human evaluation.
- CNN can reduce the time of CCTA reporting in the next future.

Journal Pre-proof



Dear Editor,

I enclose the following manuscript, entitled **“Performance of a deep learning algorithm for the evaluation of CAD-RADS classification with CCTA”**.

All authors guarantee no conflicts of interest.

Yours sincerely,

Gianluca Pontone, MD, PhD, FESC, FSCCT

Cardiologist and Radiologist

Clinical Cardiology Unit

Department of Cardiovascular Imaging

Director of MR Unit

Deputy Director of Cardiovascular CT Unit

Centro Cardiologico Monzino, IRCCS

Via Carlo Parea 4, 20138 Milan, Italy

Ph: +39 02 58002574

Fax: + 39 02 58002231

E-mail: gianluca.pontone@ccfm.it

Giuseppe Muscogiuri, Mattia Chiesa, Gianluca Pontone: Conceptualization, Methodology and Writing Original Data, Supervision.

Michela Trotta: Software

Marco Gatti, Vitano Palmisano, Serena Dell'Aversana, Francesca Baessato, Annachiara Cavaliere, Gloria Cicala, Antonella Loffreno, Giulia Rizzon: Data Curation, Data collecting and Data analysis

Marco Guglielmo, Andrea Baggiano, Laura Fusini, Luca Saba, Daniele Andreini, Mauro Pepi, Andrea Guaricci and Carlo De Cecco: Methodology

Mark G. Rabbat: Writing

Gualtiero Colombo: Supervision.

Journal Pre-proof